Journal of Alloys and Compounds 509 (2011) 7840–7843

Contents lists available at ScienceDirect

Journal of Alloys and Compounds

journal homepage: www.elsevier.com/locate/jallcom

Effect of hydrostatic pressure on martensitic transformation in a ferromagnetic shape memory alloy Ni_2MnGa

Hidefumi Maeda[a,b], Takashi Fukuda[a,*], Tomoyuki Kakeshita[a]

[a] Department of Materials Science and Engineering, Graduate School of Engineering, Osaka University, 2-1, Yamada-oka, Suita, Osaka 565-0871, Japan
[b] Department of Mechanical and Systems Engineering, Faculty of Science and Technology, Ryukoku University, Yokotani 1-5, Seta Oe-cyo, Otsu, Shiga 520-2194, Japan

ARTICLE INFO

Article history:
Received 22 April 2011
Received in revised form 9 May 2011
Accepted 11 May 2011
Available online 18 May 2011

Keywords:
Phase diagram
Volume change
Continuous transformation

ABSTRACT

Ni_2MnGa transforms in the cooling process from the parent (P-) phase to the intermediate (I-) phase and then to the martensite (M-) phase. Under a uniaxial stress, a new phase (X-phase) appears, and the P → I transformation distinctively separates to the P → X, and the X → I transformations. In the present study, we have studied the effect of hydrostatic pressure on these transformation temperatures. As a result, we found that the distinct separation described above does not occur under a hydrostatic pressure of up to 0.9 GPa. The P → X and the I → M transformation temperatures increase with increasing hydrostatic pressure, and the ratio is 13.1 K/GPa and 16.2 K/GPa, respectively. The change in molar volume and/or thermal expansion coefficient associated with the transformation is estimated from these values.

1. Introduction

Near stoichiometric Heusler-type ($L2_1$-type) Ni_2MnGa alloys have attracted much attention as new functional materials owing to their large magnetic field-induced strain [1–4] and magnetocaloric effect [5,6]. These excellent properties are closely related to magnetic transition and martensitic transformation of Ni_2MnGa. A stoichiometric Ni_2MnGa exhibits a magnetic transition near 380 K (=T_c) [7], and shows lattice softening in TA_2 branch below T_c [8,9]. The $L2_1$-type parent phase (P-phase) transforms to the so-called intermediate phase (I-phase) near 250 K [10,11], and the I-phase then transforms to the martensite phase (M-phase) having an incommensurate structure with a propagation vector $\boldsymbol{q}$ = [0.427, 0.427, 0]* (* means vector in reciprocal space) [12,13].

In addition to the P-, I- and M-phases, we reported that a new phase (X-phase) appears when a uniaxial compressive stress is applied in the [0 0 1] direction [14], and proposed the phase diagram as shown in Fig. 1. This phase diagram implies that Ni_2MnGa exhibits a successive P → X → I → M transformation under a low stress region (0 MPa < σ < 10 MPa). As the external stress increases, the X-phase region expands while the I-phase region shrinks. When the external stress exceeds about 10 MPa, the I-phase do not exist, and Ni_2MnGa undergoes a successive P → X → M transformation [15]. The diffraction pattern of the X-phase shows satellites in the ⟨1 1 0⟩* direction like the I-phase and the M-phase but their position is obviously different from those of the I- and M-phases [16].

The existence of the X-phase was also confirmed by Karaca et al. [17]. In addition, several anomalous experimental results made under compressive stress so far reported [18–20] can be well understood by considering the existence of the X-phase.

The X → M transformation is first order regardless of the strength of applied stress. The X → I transformation is also first order, but the first order nature fades out with decreasing stress [21]. Thus, under zero stress, the X- and I-phases are indistinguishable by diffraction experiments [21,22], and this will be the reason why the X-phase was not identified as a separate phase by the experiments made under zero stress so far. The P → X transformation is most likely second order, because no discontinuity is detected in physical properties between the P- and the X-phases [15].

The present study is motivated to further understand the phase relation between constituent phases (P-, I-, X- and M-phases) in Ni_2MnGa. We will examine the effect of hydrostatic pressure on the phase boundaries shown in Fig. 1. Then, from the change in transformation temperature under hydrostatic pressure, we will evaluate the change in molar volume and/or the change in volume thermal expansion coefficient associated with a transformation.

2. Experimental procedure

An ingot of stoichiometric Ni_2MnGa was prepared by arc-melting using Ni (3 N), Mn (3 N) and Ga (6 N) as starting materials. Single crystal was grown by a floating zone method under a purified argon gas flow, and it was heat-treated at 1173 K for 24 h for homogenization and then at 923 K for 24 h to obtain a highly ordered $L2_1$-type structure.

Specimens for resistivity measurements and magnetic susceptibility measurements were cut from the single crystal. Subsequently, the specimens were annealed at 1123 K for 3.6 ks in evacuated quartz tubes, and then annealed at 923 K for 86.4 ks

* Corresponding author. Tel.: +81 6 6879 7483; fax: +81 6 6879 7522.
E-mail address: fukuda@mat.eng.osaka-u.ac.jp (T. Fukuda).

0925-8388/$ – see front matter © 2011 Elsevier B.V. All rights reserved.
doi:10.1016/j.jallcom.2011.05.039

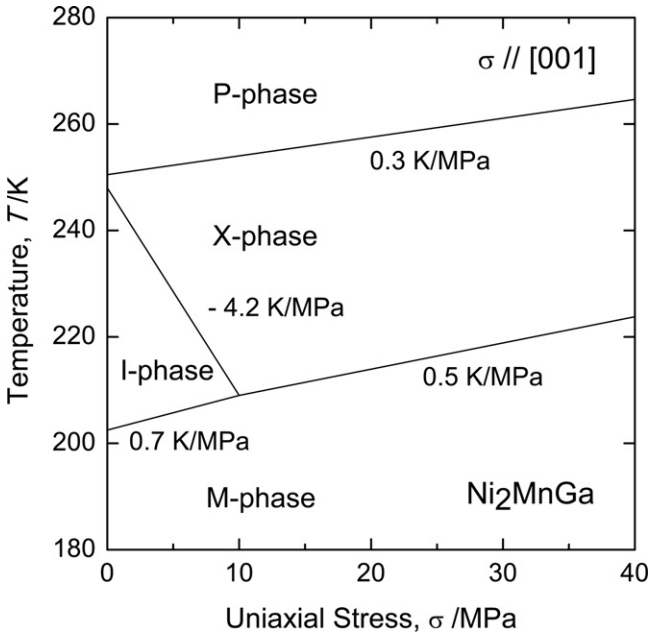

Fig. 1. Stress–temperature (σ–T) phase diagram of Ni_2MnGa under compressive stress applied in the [0 0 1] direction.

for ordering treatment followed by quenching into ice water. The surface of the specimen was electropolished in an electrolyte composed of 95 vol% CH_3COOH and 5 vol% $HClO_4$.

Martensitic transformation under a hydrostatic pressure was examined by electrical resistivity or magnetic susceptibility measurements. Electrical resistivity was measured by a four probe method and magnetic susceptibility was measured by a SQUID magnetometer. The specimens were immersed in a pressure medium (mixture of kerosene and transformer oil), and a hydrostatic pressure of up to 0.9 GPa was generated by a piston-cylinder type apparatus.

3. Results

Fig. 2 shows temperature dependence of magnetic susceptibility (χ–T curve) measured in the cooling process under hydrostatic pressures of 0 GPa, 0.2 GPa and 0.5 GPa. The measurements have

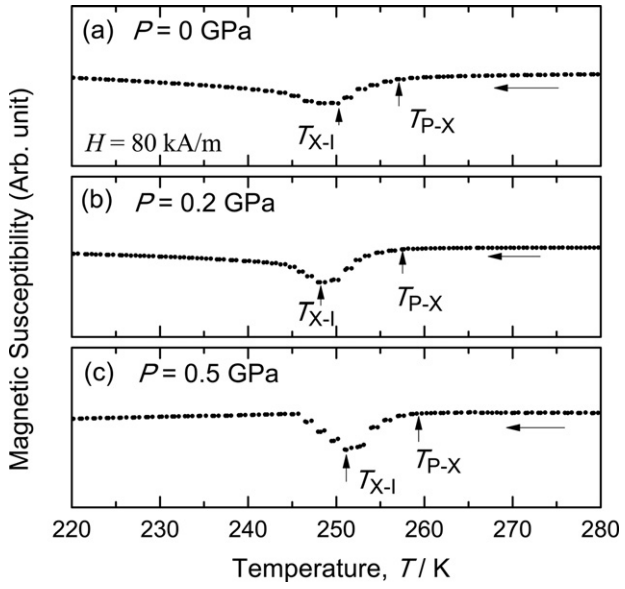

Fig. 2. Temperature dependence of magnetic susceptibility measured under hydrostatic pressures of 0 GPa (a), 0.2 GPa (b) and 0.5 GPa (c). The measurement was made by applying a low magnetic field of 80 kA/m.

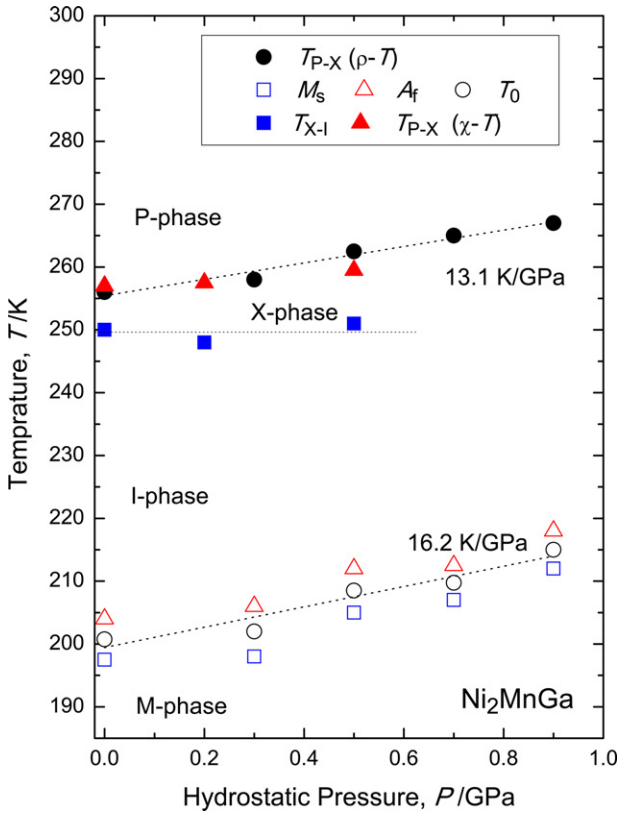

Fig. 3. Transformation temperatures plotted as a function of hydrostatic pressure (P–T phase diagram).

been made in the vicinity of temperature range for the P → X → I transformation by applying a magnetic field of 80 kA/m in the [0 0 1] direction. For all the pressures, the susceptibility in the cooling process starts to decrease at a temperature, $T_{P–X}$, as indicated with an arrow. The susceptibility then starts to increase at another temperature, $T_{X–I}$, as indicated by another arrow. The decrease in susceptibility is due to the P → X transformation and the increase in susceptibility is due to the X → I transformation, according to previous studies of stress–strain curve [14,15] and neutron diffraction [16]. Both $T_{P–X}$ and $T_{X–I}$ are plotted as a function of hydrostatic pressure in Fig. 3. We notice that $T_{P–X}$ increases with increasing hydrostatic pressure while $T_{X–I}$ is almost independent of hydrostatic pressure. Similar hydrostatic pressure dependence of magnetic susceptibility curve was reported by Chernenko et al. [23] although the existence of the X-phase was not described there.

We have measured temperature dependence of electrical resistivity (ρ–T curve) under a hydrostatic pressure ($0 \le P \le 0.7$ GPa), and typical results ($P = 0$ and 0.7 GPa) are shown in Fig. 4. As known from the figure, there is a bend point as indicated by a double arrow, and the temperature of the bend point is plotted by solid circles as a function of hydrostatic pressure in Fig. 3. We notice that the bend point in ρ–T curve is in good agreement of the $T_{P–X}$, obtained by χ–T curve. So, we interpret this bend point corresponds to the P → X transformation temperature. The temperature $T_{P–X}$, increases linearly with increasing hydrostatic pressure, and the gradient is 13.1 K/GPa. Incidentally, the X → I transformation, which can be detected by magnetic susceptibility measurements, cannot be detected by electrical resistivity measurements.

On further cooling, the resistivity shows an increase as indicated by a single arrow in Fig. 4. This increase is due to the initiation of the I → M transformation, and we denote this temperature as M_S. In the subsequent heating process, the heating curve merges the cooling curve at the temperature indicated by another arrow. The merge is

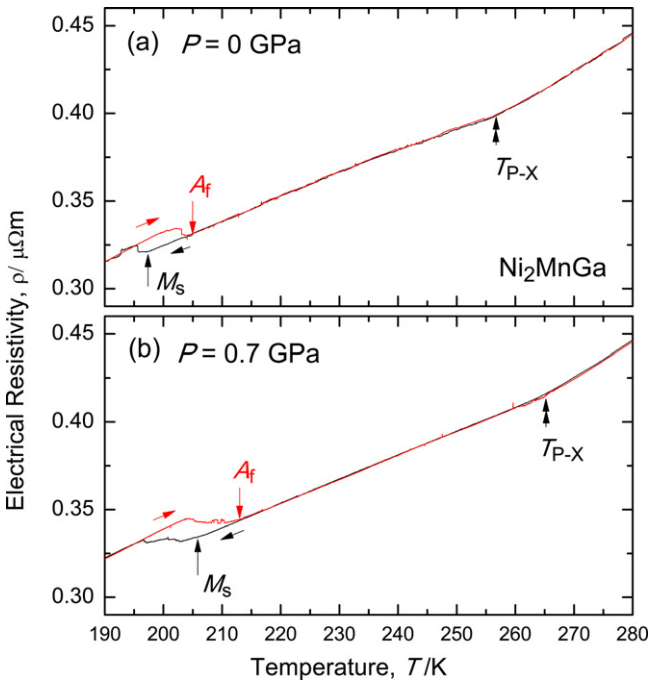

Fig. 4. Temperature dependence of electrical resistivity measured under hydrostatic pressures of 0 GPa (a) and 0.7 GPa (b).

due to the termination of the M → I transformation, and we denote this temperature as A_f. We define the equilibrium temperature for the I → M transformation as $T_0 = (M_s + A_f)$ after Tong and Wayman [24]. The temperatures M_s, A_f and T_0 are plotted as a function of hydrostatic pressure in Fig. 3. We notice that T_0 increases with increasing hydrostatic pressure, and the gradient is 16.2 K/GPa. This gradient is the same order as that reported for $Ni_{50}Mn_{36}Sn_{14}$ [25] and $Ni_{49.5}Mn_{35.5}In_{15}$ [26].

4. Discussion

In this section, we discuss the volume change or change in volume thermal expansion coefficient using the gradient of phase boundary shown in Fig. 3.

First, we discuss the volume change for the I → M transformation. Since the I → M transformation is first order, the hydrostatic pressure, P, dependence of the equilibrium temperature T_0 should satisfy the Clausius–Claperyron equation,

$$\frac{dT_0}{dP} = \frac{\Delta V}{\Delta S} \quad (1)$$

Here ΔV is the difference in molar volume and ΔS is the difference in molar entropy between the M-phase and the I-phase at T_0. The value of ΔS at T_0 (~200 K) is obtained to be −0.465 J/mol K from the latent heat of −93 J/mol reported for this alloy [27]. Putting this value and the gradient $dT/dP = 16.2$ K/GPa into the above equation, we obtain $\Delta V = -7.5 \times 10^{-9}$ m^3/mol. The molar volume of the I-phase is calculated to be about $V_I = 7.4 \times 10^{-6}$ m^3/mol from its lattice parameters [28]. Then we obtain $\Delta V/V_I = -1.0 \times 10^{-3}$, meaning that Ni_2MnGa contracts by 0.10% in volume in association with the I → M transformation. This volume change is the same order as that of the P → 2M and the P → 14M transformations in Ni–Mn–Ga alloys [29], which implies the validity of the present experimental result of hydrostatic pressure dependence of martensitic transformation temperature. Incidentally, in order to evaluate such a small volume change from the change in lattice parameters, the value of lattice parameters should be given in the precision of five digits for both the I- and M-phases, but there is no available experimental result of lattice parameters evaluated in such a high precision. Thus, hydrostatic pressure is effective for determining the volume change associated with martensitic transformation.

Next, we discuss the change in volume thermal expansion coefficient for the P → X transformation. Since the P → X transformation is second order like, the hydrostatic pressure dependence of the transformation temperature will satisfy the Ehrenfest equation,

$$\frac{dT}{dP} = \frac{T\Delta\beta}{\Delta C_p} \quad (2)$$

Here ΔC_p is the difference in specific heat and $\Delta\beta$ is the difference in volume thermal expansion coefficient between the I- and P-phases. Temperature dependence of specific heat for Ni_2MnGa was reported by Opel et al. [30], and we can read the value of ΔC_p to be about −1.0 J/mol (−1.35 × 10^4 J/m^3). Putting this value and $dT/dP = 13.1$ K/GPa in Fig. 3, we obtain $\Delta\beta$ to be -6.9×10^{-7}/K. Wu and Finlayson [18] measured the linear thermal expansion coefficient of Ni_2MnGa, and we can read the value for the P-phase to be $\alpha_P = 1.7 \times 10^{-5}$/K. Then the volume thermal expansion coefficient of the P-phase is $\beta_P = 3\alpha_P = 5.1 \times 10^{-5}$/K. Consequently, the ratio $\Delta\beta/\beta_P$ is calculated to be −0.013, meaning that the volume expansion coefficient decreases by 1.3% in association with the P → X transformation.

Finally we discuss the volume change for the X → I transformation. By comparing the P–T phase diagram shown in Fig. 3 with the σ–T phase diagram shown in Fig. 1, we notice that there is a significant difference in the I–X phase boundary. That is, the significant extension of the X-phase region under uniaxial stress does not occur under hydrostatic pressure. This difference implies that the X-phase region is expanded essentially by the shear component of the uniaxial stress, and the volume change for the I–X transformation is negligibly small. We can roughly estimate the volume change using Eq. (1). The latent heat for the X → I transformation is smaller than 7 J/mol according to references [11,21], so the entropy change is smaller than 30 mJ/mol K. On the other hand, $|dT/dP|$ is nearly zero from Fig. 2, and does not exceed 5 K/GPa no matter how we take the gradient in Fig. 2. Then the volume change for the X → I transformation comes to be smaller than 2×10^{-10} m^3/mol, and $|\Delta V/V|$ is smaller than 3×10^{-5}, being two order in magnitude smaller than that for the I → M transformation.

5. Conclusions

We have constructed pressure–temperature phase diagram of Ni_2MnGa. The I → M transformation temperature increases with increasing hydrostatic pressure (16.2 K/GPa), and the volume change of the transformation is estimated to be contraction of 0.10%. The P → I transformation temperature also increases with increasing hydrostatic pressure (13.1 K/GPa), and the change in volume thermal expansion coefficient is estimated to be a decrease in 1.3%. On the other hand, influence of hydrostatic pressure on the X → I transformation is negligibly small, and the volume change for the X → I transformation is two order in magnitude smaller than that for the I → M transformation.

Acknowledgement

This work was supported by the Global COE program "Center of Excellence for Advanced Structural and Functional Design" by MEXT Japan.

References

[1] K. Ullakko, J.K. Huang, C. Kantner, R.C. O'Handley, V.V. Kokorin, Appl. Phys. Lett. 69 (1996) 1966–1968.
[2] S.J. Murray, M. Marioni, S.M. Allen, R.C. O'Handley, T.A. Lograsso, Appl. Phys. Lett. 77 (2000) 886–888.

[3] A. Sozinov, A.A. Likhachev, N. Lanska, K. Ullakko, Appl. Phys. Lett. 80 (2002) 1746–1748.
[4] P. Müllner, V.A. Chernenko, M. Wollgarten, G. Kostorz, J. Appl. Phys. 92 (2002) 6708–6713.
[5] J. Marcos, L. Mañosa, A. Planes, F. Casanova, X. Batlle, A. Labarta, Phys. Rev. B 68 (2003) 944011–944016.
[6] V.V. Khovaylo, K.P. Skokov, O. Gutfleisch, H. Miki, R. Kainuma, T. Kanomata, Appl. Phys. Lett. 97 (2010) 052503.
[7] P.J. Webster, K.R.A. Ziebeck, S.L. Town, M.S. Peak, Philos. Mag. B 49 (1984) 295–310.
[8] A. Zheludev, S.M. Shapiro, P. Wochner, L.E. Tanner, Phys. Rev. B 54 (1996) 15045–15050.
[9] U. Stuhr, P. Vorderwisch, V.V. Kokorin, P.-A. Lindgård, Phys. Rev. B 56 (1997) 14360–14365.
[10] V.V. Kokorin, V.A. Chernenko, E. Cesari, J. Pons, C. Segui, J. Phys.: Condens. Matter 8 (1996) 6457–6463.
[11] A. Planes, E. Obrandó, E.A. Gonzàlez-Comas, L. Moñosa, Phys. Rev. Lett. 79 (1997) 3926–3928.
[12] L. Righi, F. Albertini, G. Calestani, L. Pareti, A. Paoluzi, C. Ritter, P.A. Algarabel, L. Morellon, M.R. Ibarra, J. Solid State Chem. 179 (2006) 3525–3533.
[13] H. Kushida, K. Fukuda, T. Terai, T. Fukuda, T. Kakeshita, T. Ohba, T. Osakabe, K. Kakurai, K. Kato, Eur. Phys. J. 158 (2008) 87–92.
[14] J.-h. Kim, T. Fukuda, T. Kakeshita, Scripta Mater. 54 (2006) 585–588.
[15] H. Kushida, K. Hata, T. Fukuda, T. Terai, T. Kakeshita, Scripta Mater. 60 (2009) 96–99.
[16] H. Kushida, T. Terai, T. Fukuda, T. Kakeshita, T. Osakabe, K. Kakurai, Scripta Mater. 60 (2009) 248–250.
[17] H.E. Karaca, I. Karaman, B. Basaran, D.C. Lagoudas, Y.I. Chumlyakov, H.J. Maier, Acta Mater. 55 (2007) 4253–4269.
[18] X.D. Wu, T.R. Finlayson, J. Phys.: Condens. Matter 19 (2007) 02618.
[19] A. Zheludev, S.M. Shapiro, Solid State Commun. 98 (1996) 35–39.
[20] A. Gonzàlez-Comas, E. Obradó, L. Mañosa, A. Planes, V.A. Chernenko, B.J. Hattink, A. Labarta, Phys. Rev. B 60 (1999) 7085–7090.
[21] T. Fukuda, T. Terai, H. Kushida, T. Kakeshita, T. Osakabe, K. Kakurai, Philos. Mag. 90 (2010) 1925–1935.
[22] T. Fukuda, H. Kushida, M. Todai, T. Kakeshita, H. Mori, Scripta Mater. 61 (2009) 473–476.
[23] V.A. Chernenko, S. Besseghini, T. Kanomata, H. Yoshida, T. Kakeshita, Scripta Mater. 55 (2006) 303–306.
[24] H.C. Tong, C.M. Wayman, Acta Metall. 23 (1975) 209–215.
[25] X. Moya, L. Mañosa, A. Planes, T. Krenke, E. Duman, M. Achet, E.F. Wassermann, J. Magn. Magn. Mater. 316 (2007) e572–e574.
[26] L. Mañosa, X. Moya, A. Planes, O. Gutfleisch, J. Lyubina, S. Aksoy, T. Krenke, M. Acet, Appl. Phys. Lett. 92 (2008) 012515.
[27] J.-h. Kim, F. Inaba, T. Fukuda, T. Kakeshita, Acta Mater. 54 (2006) 493–499.
[28] T. Ohba, N. Miyamaoto, K. Fukuda, T. Fukuda, T. Kakeshita, K. Kato, Smart Mater. Struct. 14 (2005) S197–S200.
[29] J.-h. Kim, T. Taniguchi, T. Fukuda, T. Kakeshita, Mater. Trans. 46 (2005) 1928–1932.
[30] C.P. Opel, B. Mihaila, R.K. Schulze, L. Mañosa, A. Planes, W.L. Hults, R.A. Fisher, P.S. Riseborough, P.B. Littlewood, J.L. Smith, J.C. Lashley, Phys. Rev. Lett. 100 (2008) 165703.